Surface analysis of WC-5%Co cemented tungsten carbide cutting insert after plunge-face grinding

Dennis Coelho Cruz
Department of Materials Engineering, Federal University of São Carlos, Rod. Washington Luís km 235, 13565-905 São Carlos, SP, Brazil
denniscoelhocruz@gmail.com

Vitor Luiz Sordi
Department of Materials Engineering, Federal University of São Carlos, Rod. Washington Luís km 235, 13565-905 São Carlos, SP, Brazil
sordi@ufscar.br

Carlos Eiji Hirata Ventura*
Department of Mechanical Engineering, Federal University of São Carlos, Rod. Washington Luís km 235, 13565-905 São Carlos, SP, Brazil
ventura@ufscar.br

*Corresponding author: E-mail: ventura@ufscar.br, Phone: +55 16 3306-6857

Abstract

In order to improve surface and edge quality of cemented tungsten carbide cutting inserts, a well-designed grinding process should be applied. Efficiency and good insert integrity are only possible when cutting parameters and grinding wheel are correctly chosen and, for this, the comprehension of the process plays an important role. Within this context, this work brings an experimental investigation of plunge-face grinding of WC-5%Co cutting inserts, evaluating surface roughness, edge quality and specific energy in terms of chip thickness, which changes not only with cutting conditions (cutting and feed speed), but also with grinding wheel bonding material (vitrified and resin). Higher values of chip thickness, obtained with higher feeds, lower cutting speeds and a vitrified binder, led to a predominantly brittle material removal, reducing specific energy, but damaging surface quality. Otherwise, edge roughness was not influenced by different grinding conditions within the studied range.

Keywords: plunge-face grinding, cemented tungsten carbide, cutting insert, surface integrity

1. Introduction

In order to increase tool life during its application in metal cutting operations, the cutting insert is ground after sintering to avoid irregularities and to improve the surface finish of rake and flank faces, as well as edge quality. Sharp edges are generated from the intersection of these two surfaces and thus, depend on the applied grinding process. Rake faces are usually machined by double side-face grinding, while flank faces are finished by plunge-face grinding.

In grinding of brittle materials, chip removal takes place predominantly through the formation of radial and lateral micro cracks. Lateral cracks are responsible for the effective material removal, whilst radial cracks damage the surface layer [1]. However, Bifano et al. demonstrated that such materials can experience a ductile removal when chip thicknesses lower than a critical value are applied [2]. In this direction, Dai et al. carried out grinding tests with a single diamond grain in a SiC ceramic and demonstrated through surface and subsurface analyses that the transition from ductile to a brittle material removal is related to a critical uncut chip thickness, from which lower and stable values of specific energy are obtained [3]. Wu et al. modeled the surface roughness of this same material considering the simultaneous effect of brittle and ductile material removal modes. More stable and lower values of surface roughness were obtained when ductile mode was predominant, while the opposite was observed for brittle material removal, which plays a more important role in the surface quality of brittle materials [4].

In addition to crack formation, in grinding of cemented tungsten carbides with diamond grinding wheels, rupture and fragmentation of the material grains are also observed. Part of the carbide grains is removed, causing disruption in the surface. The other part is compressed and plastically deformed by the abrasive grains of the grinding wheel. The bond of cemented tungsten carbide is in part compressed with the fragmented carbides and in part removed [5, 6]. Yang et al. detected microcracks and smeared binder after grinding WC-Co with a diamond wheel considering an industrial protocol. They noted that in the subsurface of the ground specimen there is a Co transformation from the original fcc to a more stable hcp phase. However, such transformation is reversed by high temperatures and the volume change related to this process can lead to the formation of microvoids in the binder [7]. In a further study, Yang et al. suggested that the deformation of Co changes the local stress concentration during the penetration of the abrasive grain in grinding and contributes to crack nucleation [8].

Takeyama et al. observed that larger WC grains increase the probability of microfracture at the grain boundary, due to the higher stresses in the binder phase or in the grain boundary. Plastic flow of the binder phase triggers microdefects, such as microfracture at the grain boundaries and fall-off of the WC grains [9]. Hegeman et al. mentioned that the intensity of pull out and fragmentation of tungsten carbide grains is higher for smaller grain sizes, while larger WC grains are normally cracked during grinding [5]. On the contrary, after ultraprecision grinding of cemented carbide specimens with different grain sizes and cobalt content, Yin et al. did not find evidence

of WC grain fracture or fragmentation, but only microgrooves in the carbide phases. Thus, they concluded that plastic flow dominated the removal process, probably because of the reduced uncut chip thickness [10]. In single grain scratch tests, Klocke et al. noted five different stages with the increase in depth of cut: (1) cracks within WC grains, (2) disruption, (3) block building, (4) material flaking and (5) breakouts. This latter condition was considered a limit from which material behavior changes from predominantly ductile to predominantly brittle. An increase in this critical depth can be achieved by higher values of cobalt (Co) content [11].

Ren et al. obtained the specific energy during grinding of cemented tungsten carbide workpieces with different WC grain sizes. In all cases, a decrease in chip thickness led to an increase in specific energy, which was attributed to the size effect, i.e., smaller volumes of removed material have a lower probability of presenting microstructural defects, like dislocations or grain boundaries. This increases material strength and reduces cutting efficiency [6]. According to Badger, sub micro grade WC-Co presents a size effect similar to brittle materials, being most of the specific energy caused by ploughing [12].

Zhan and Xu investigated heat partition during dry diamond grinding of cemented carbide and observed that the reduction of undeformed chip thickness with the increase in wheel speed leads to a more ductile material removal and demands more energy. Accordingly, the heat generated increases and, consequently, the temperature. Additionally, they noted that higher values of depth of cut increase material removal rate and, as a result, cutting temperature. Otherwise, the increase in feed rate reduces the period the heat source acts on the workpiece, decreasing its temperature [13]. After diamond grinding cemented carbide ISO grade P25 specimens, Biermann and Würz observed that an increase in cutting speed leads to an increase in thermal energy, which causes cracks on the ground surface. However, an increase in the number of active edges and a consequent reduction of average chip thickness, caused by higher values of cutting speed, contributes to a decrease in surface roughness [14]. Yin et al. affirmed that the reduction of chip thickness to a nano scale in diamond grinding of a fine grained WC-Co composite reduces surface roughness significantly, creating a fracture-free mirror like surface [15].

In grinding of a sub micro grade WC-Co with a resin bonded wheel, Badger noted the occurrence of wheel loading. He affirms that the intensity of the loading is not directly related to Co, but may be due to the nature of the chips, which are shorter and blockier than chips produced by ductile materials [12]. Abdullah et al. did not investigate the topography of the grinding wheel after diamond grinding a WC-20%Co alloy, but their experiments showed that an increase in cutting speed causes a decrease in chip thickness and a consequent decrease in cutting force. This leads to a reduction of profile wear. Based on the same explanation, a contrary trend is observed with the increase in feed rate, what generates thicker chips [16]. Habrat evaluated the normal and tangential force components in grinding of cemented tungsten carbide with metal and resin bonded grinding wheels and noted that this latter led to significantly lower force values [17], probably because of the reduced friction between wheel and workpiece.

All the described works are related to cylindrical or face grinding and consider neither the influence of the grinding wheel bonding material on chip thickness nor the edge quality as an output variable. Thus, considering the particular process kinematics and the importance of surface and edge quality when finishing cutting inserts, this paper analyzes aspects of grinding cutting inserts composed of WC-5%Co cemented tungsten carbide. Output variables like surface and edge roughness, as well as specific energy, are evaluated with regard to the variation of chip thickness, which is calculated with basis on the characteristics of grinding wheel topography.

2. Experimental procedure

Cemented tungsten carbide cutting inserts with composition WC-5%Co (grain size ~1.3 µm) and dimensions 12.6 mm × 12.6 mm × 4.7 mm (SNMN1204-) had their flank faces ground with flood coolant (mineral oil) in a 4-axes CNC grinding machine for insert preparation Agathon DOM Plus (Figure 1), with maximum power of 16 kW and maximum rotation speed of 3400 min^{-1}.

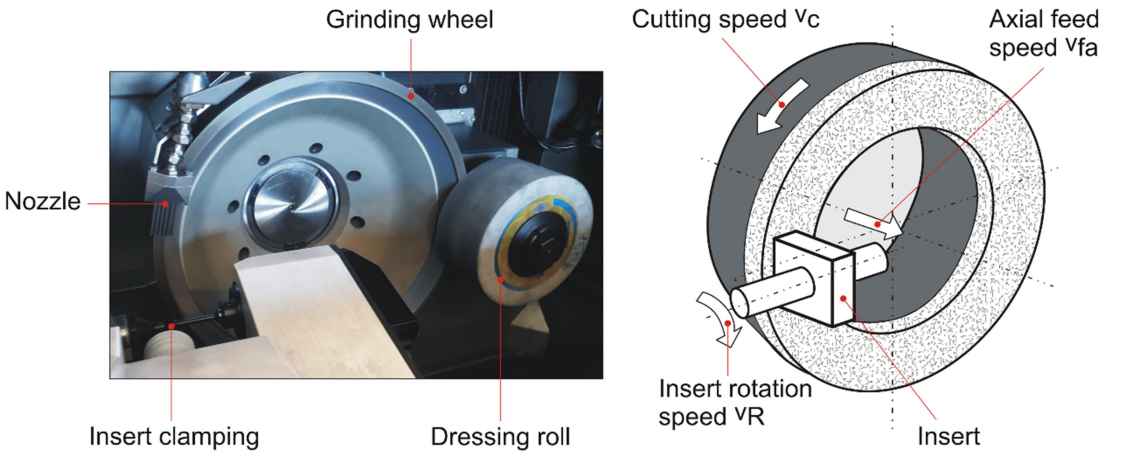

Fig. 1 Grinding machine for insert preparation used in the experiments

Different wheel bonding materials have distinct impacts on workpiece quality, as they influence grain protrusion, the number of active cutting edges and elastic deflection of the system during grinding. Resin binders have increased ability to retain abrasive grains and contribute to increase the number of active edges, but can damage dimensional tolerances, due to its elastic deformation. Differently, vitrified binders are more rigid, but tend to release abrasive grains and reduce the number of active edges, what can damage surface roughness. Thus, diamond cup grinding wheels with grain size of 46 µm, concentration C100, resin and vitrified binder were tested. Such grain size and abrasive concentration were chosen due to their wide use by cemented carbide parts manufacturers.

Before grinding each insert (material removal of approximately 20 mm^3), wheel conditioning was performed with a cup dressing wheel of alumina and grain size 180 mesh. In this latter process, the tangential speed of the grinding wheel, the tangential

speed of the dressing wheel and the dressing feed were kept constant, with values v_c = 20 m/s, v_{cd} = 10 m/s, and v_{fd} = 3 μm/s, respectively.

The range of grinding parameters was chosen considering the values commonly used in commercial processes and the limits of the machine. Regarding to this, the tests were performed in a partial factorial design, according to Table 1. Taking the process kinematics into account, the depth of cut corresponds to the insert width b = 4.7 mm and is kept constant. The wheel wear during grinding of one insert can be neglected and thus each side of the square insert is considered as a test repetition.

Table 1 Grinding experiments

Test	Cutting speed v_c [m/s]	Axial feed speed v_{fa} [mm/min]	Wheel binder
1	12		Resinoid
2	20	6	
3	40		
4		2	
5	20	6	
6		12	
7	12		Vitrified
8	20	6	
9	40		
10		2	
11	20	6	
12		12	

To calculate the specific energy (power / material removal rate) for the distinct process conditions, tangential force component was obtained through a force measuring system based on the measurement of the motor electric current, with an acquisition rate of 50 Hz. Such system and the correspondent acquisition software are integral part of the machine and were developed by its manufacturer, therefore, further details are confidential.

After each test, insert integrity and grinding wheel topography were assessed by means of a confocal microscope Alicona InfiniteFocus SL. Wheel topography was evaluated through *Spk* (reduced peak height in area – parameter from the Abbott-Firestone curve, which gives a measure of the grain protrusion) and *Smr1* (fraction of the abrasive surface, which consists of peaks above the core material). Two different areas of the wheel abrasive layer with 4 mm^2 were analyzed and average values were used for the discussion.

Insert integrity was evaluated through the same microscope by measuring edge chipping Δr (minimum distance between an ideal edge and its real contour, Figure 2a) and surface roughness parameters perpendicular to grinding direction at the flank face (Figure 2b): *Rz* (average value of maximum peak-valley distances in five different parts of a roughness profile), *Rpk* (reduced peak height from the Abott-Firestone curve), *Rvk* (reduced valley depth from the Abott-Firestone curve), *Rsk* (skewness) and *Rku* (kurtosis). The parameter *Rz* provides a general description of the roughness profile,

while *Rpk* and *Rvk* give a measure of peaks and valleys beyond the core roughness, separately. These three factors contribute to understand the influence of grinding process on the formation of surface irregularities. The parameters *Rsk* and *Rku* were chosen to measure the asymmetry and flattening/sharpening of the roughness profile distribution and are relevant to characterize load bearing capacity and wear resistance. The parameter *Δr* is commonly used as a measure of edge quality, being higher values related to larger chippings.

Average values of all roughness parameters calculated from 100 profiles at each insert side (= 400 roughness profiles) and average values of *Δr* calculated from 150 measurements per insert side (= 600 measurements) were used for the analysis. The rake faces of the cutting inserts received all the same grinding treatment and have a roughness value $Rz = 1.34 \pm 0.05$ μm.

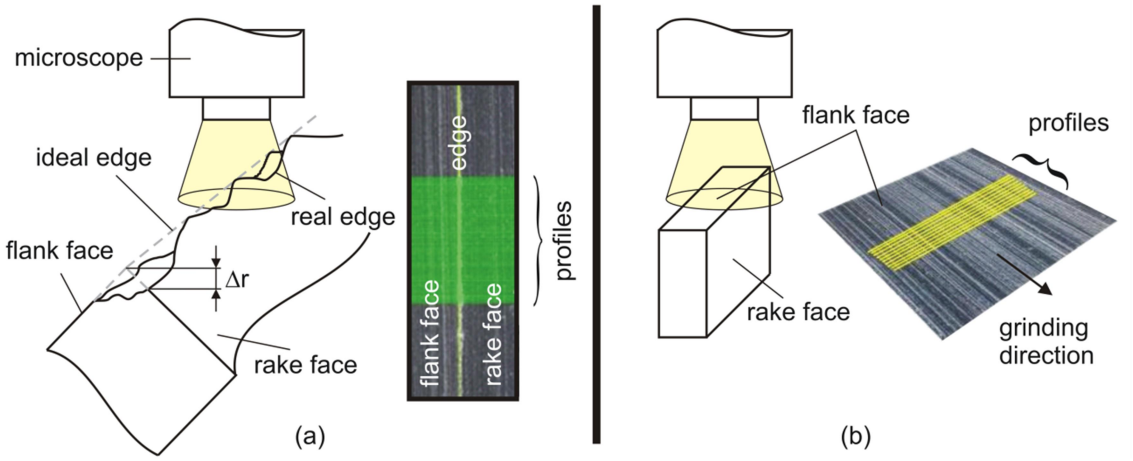

Fig. 2 Measurement of (a) edge chipping *Δr* and (b) surface roughness parameters

3. Considerations about single grain chip thickness

Friemuth [18] developed an average single grain chip thickness model to be applied in plunge-face grinding with the goal of obtaining a characteristic value to consider the influence of different grinding parameters on output variables, like specific energy, surface and edge roughness. The approach was based on the continuity equation, an estimation of the number of active cutting edges, and hypotheses related to the absence of cutting overlap, elastic deflection and grit wear. Abrasives with spherical form were also considered, based on the stable form that diamond grains assume during grinding of hard materials.

The number of active cutting edges in the abrasive layer was obtained from the nominal volumetric concentration of abrasives and an estimation of the grain protrusion, but does not consider the actual number of edges, which can vary during the process, depending on the binder's ability to retain the abrasive grains. Considering this, in the present work the grinding wheel topography was analyzed after grinding each insert and the concentration was corrected based on the measurement of the fraction of the surface, which consists of peaks above the core material (*Smr1*). Irrespective of the applied

cutting conditions, only few or no pores were found in the abrasive layer of the resin bonded grinding wheel (Figure 3a), differently of the vitrified bonded grinding wheel, in which voids and pores can be noted (Figure 3b). This leads to a *Smr1* value approximately 70% lower. Thus, a correction factor $fc = 0.7$ was used to adequate the number of active edges of the vitrified bonded grinding wheel in relation to the resin bonded wheel.

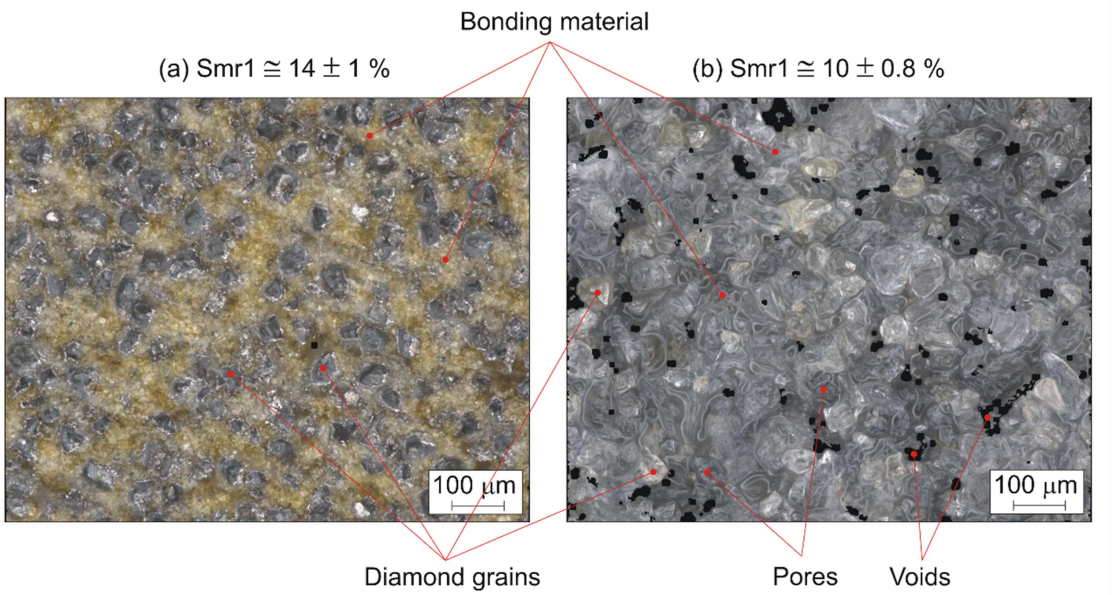

Fig. 3 Images of the abrasive layer of (a) resin and (b) vitrified bonded grinding wheels

Bearing this in mind and based on the work of Friemuth [18], Equation 1 can be used to calculate average single grain chip thickness h_{cu} for different conditions in plunge-face grinding.

$$h_{cu} = \left(\frac{1}{C_2+1}\right)^{\frac{1}{C_2}} \cdot \left[\frac{(C_2+1)\cdot v_{fa}}{N_{GV}\cdot fc\cdot C_1\cdot v_c}\right]^{\frac{1}{C_2+1}} \quad (1),$$

with $C_1 = 4/3 \times (d_G)^{1/2}$, $C_2 = 1.5$ (factors used to calculate grain geometry), d_G = average grain size, v_{fa} = axial feed speed, v_c = cutting speed, N_{GV} = number of edges / volume, *fc* = correction factor (1 for resinoid and 0.7 for vitrified binder).

4. Results and discussion

The different values of *Spk* in the abrasive layer give a measure of the grain protrusion and can be related to the wear of the abrasive grains or the bonding material. Within this context, alterations of the grinding wheel topography (quantified by *Spk*) due to grinding were related to the single grain chip thickness in each situation and can be observed in Figure 4. The horizontal ranges are positioned in the average values of *Spk* after dressing and their widths correspond to their standard deviations.

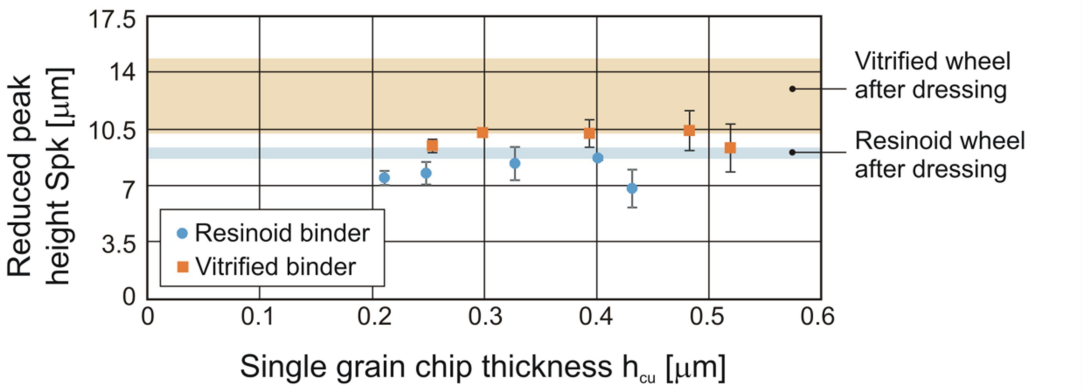

Fig. 4 Reduced peak height measured in the abrasive layer after grinding with different conditions

The parameter *Spk* did not change significantly for the different conditions, although lower values in comparison to the dressed wheel are noted, which are related to the first wear stage of the grinding wheel, when sharp edges contribute to stress concentration and are easily broken. For the resin bonded grinding wheel, an average value of 7.82 µm was obtained, while for the vitrified bonded wheel, an average value of 9.94 µm. Higher values in this latter case are related to the presence of pores, which decrease the level of the core material and increase the exposure of the grains. Low values of standard deviation verify the homogeneity of the grinding wheel abrasive layer.

The influence of grinding parameters on the insert quality is demonstrated in Figure 5. Figure 5a to Figure 5e show distinct surface roughness parameters in function of different values of single grain chip thickness, while Figure 5f shows the behavior of edge roughness. An increase in single grain chip thickness leads to higher mechanical loads and causes deeper grooves on the surface, what tends to increase roughness. This can be observed with the evolution of *Rz*, *Rpk* and *Rvk*, in Figures 5a, 5b and 5c, respectively. It is noteworthy that the behavior of *Rz* is more similar to that observed for *Rvk*, which means that an increase in surface roughness is closer related to deeper valleys. A smoother growth of *Rpk* indicates that ploughing and smearing of the ground material do not play the most important role in roughness of ground cemented tungsten carbide. Nevertheless, the differences and variations of the presented parameters were not enough to significantly affect the symmetry (skewness $Rsk \cong 0$, Figure 5d) and normal distribution (kurtosis $Rku \cong 3$, Figure 5e) of the profiles, which did not change with chip thickness or grinding wheel binder, results supported by the homogeneous abrasive wheel layer. Considering the application of the ground insert, these latter roughness parameters point to a regular and adequate surface, without the presence of sharp peaks or valleys, contributing to an increase in load bearing and coating adhesion capacity.

The edge roughness corresponds to a combination of roughness profiles obtained in two different surfaces (flank and rake faces) and should follow the same trend, considering that rake faces have all the same grinding treatment. However, a lower backing effect of the WC grains embedded in the Co binder causes their irregular

removal. This leads to a large dispersion of data and the absence of a clear trend between edge roughness and chip thickness (Figure 5f).

It should be pointed out that inserts with chip breaker are commonly produced by hot isostatic pressing and have their rake faces not ground, what can influence the levels of edge chipping after plunge-face grinding of the flank faces.

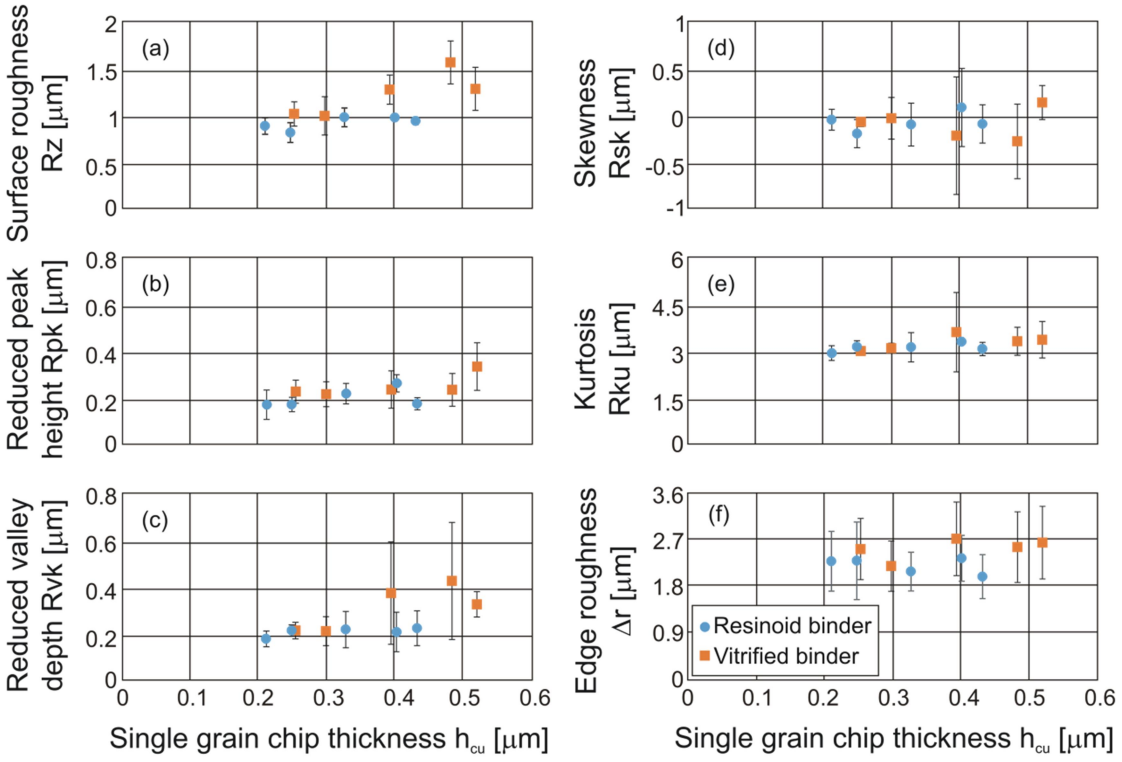

Fig. 5 Influence of single grain chip thickness on surface roughness parameters (a) *Rz*, (b) *Rpk*, (c) *Rvk*, (d) *Rsk*, (e) *Rku* and (f) edge chipping (*Δr*)

Optical images of the insert edges (2 mm length) after grinding with different conditions are shown in Figure 6. Large edge chippings can be observed in all cases, irrespective of the grinding conditions and wheels applied.

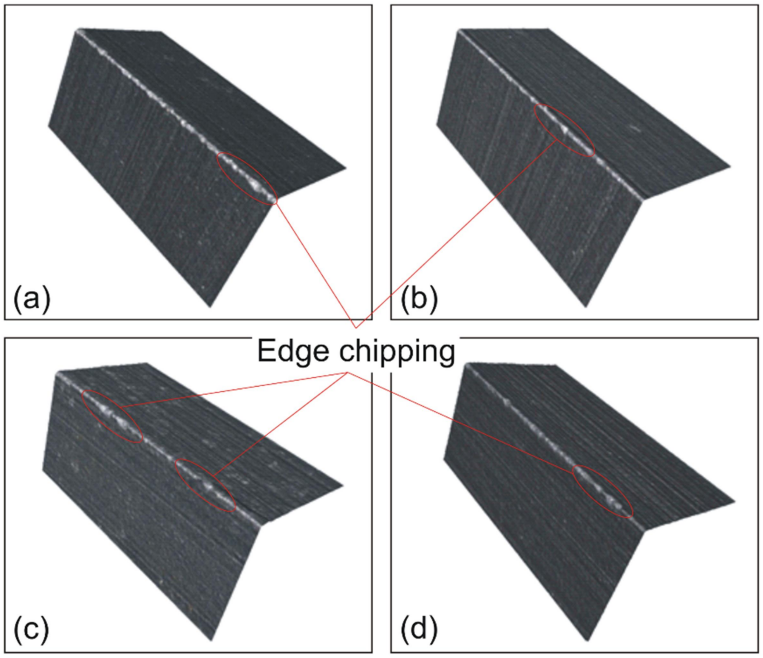

Fig. 6 Optical images of insert edges ground with (a) h_{cu} = 0.25 µm, resin bonded grinding wheel, (b) h_{cu} = 0.30 µm, vitrified bonded grinding wheel, (c) h_{cu} = 0.40 µm, resin bonded grinding wheel, (d) h_{cu} = 0.48 µm, vitrified bonded grinding wheel

Different wheel binder materials affect not only the number of active edges in the wheel layer, but also the contact behavior between grinding wheel and cemented carbide insert. In comparison to resinoid binder, vitrified binder should increase friction and, consequently, temperature, damaging the insert edges and surfaces. This explains the slightly higher values of Rz and Δr obtained with the vitrified grinding wheel. Moreover, its low ability to retain the diamond grains in the abrasive layer makes the process more unstable and leads to higher values of standard deviation, as it can be observed in Figure 5.

Subsequent processes, like edge preparation or coating, can be applied to avoid the negative effects of edge chipping, contributing to the reduction of stress concentration and increase of edge strengthening. Regarding to this, lower values of Δr enable the preparation of smaller edge radii and a more regular coating deposition, with increased adhesion. This can lead not only to a reduction of the time spent on other processes, but also to an increase in tool life.

Cemented tungsten carbide is a composite material, which consists of hard grains of WC and a soft binder phase of Co. The combination of both results in a complex behavior in terms of material deformation and removal, according to the SEM images of ground surfaces, depicted in Figure 7. Radial cracks occur for small and large chip thicknesses, but an irregular material removal is noted in Figure 7c and 7d (higher h_{cu}), where deeper grooves, smearing of Co binder, and pullout of clusters of WC grains are evident. Similar results were reported by Hegeman et al. [5] with coarser grinding wheels.

Otherwise, shallower grooves, a more effective shearing of the material and a regular surface are observed in Figures 7a and 7b (lower h_{cu}). As reported in Figure 5, rather small differences are noted for surfaces produced with different grinding wheels.

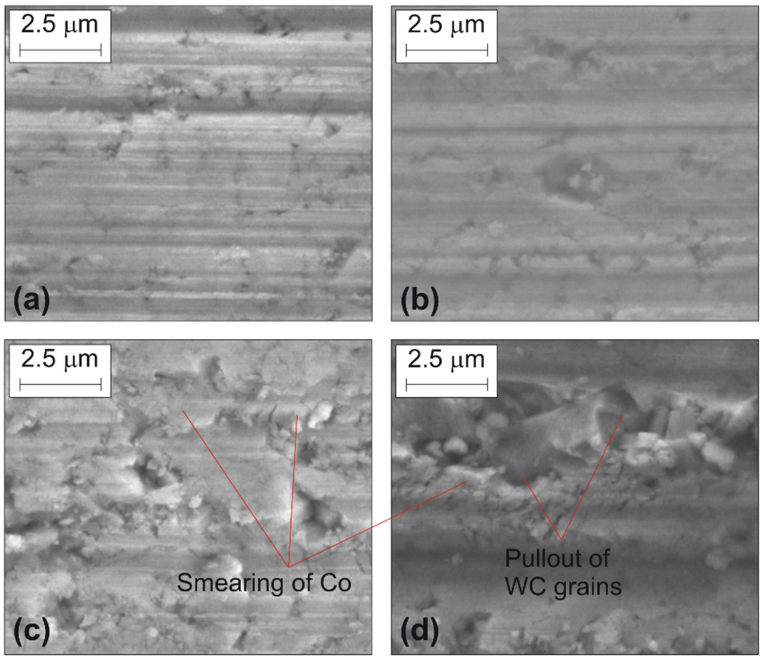

Fig. 7 SEM images of insert flank faces ground with (a) h_{cu} = 0.25 µm, resin bonded grinding wheel, (b) h_{cu} = 0.30 µm, vitrified bonded grinding wheel, (c) h_{cu} = 0.40 µm, resin bonded grinding wheel, (d) h_{cu} = 0.48 µm, vitrified bonded grinding wheel

The improvement of surface roughness with the application of smaller single grain chip thicknesses can be related to a brittle-ductile transition. According to Bifano et al. [2], brittle materials tend to be machined in a ductile regime when chip thickness is lower than a critical value. In this case, high compressive stresses plastically deform the material before it shears, improving the surface quality in comparison to brittle removal, when material separation occurs mainly through crack formation.

The increase in specific energy with lower chip thickness values (Figure 8) demonstrates that higher energy is consumed for plastic deformation before shearing, whilst lower energy is necessary for crack propagation. The graph still shows that specific energy becomes approximately constant after a critical chip thickness of ~0.4 µm, from which material removal tends to a brittle behavior and surface roughness deteriorates.

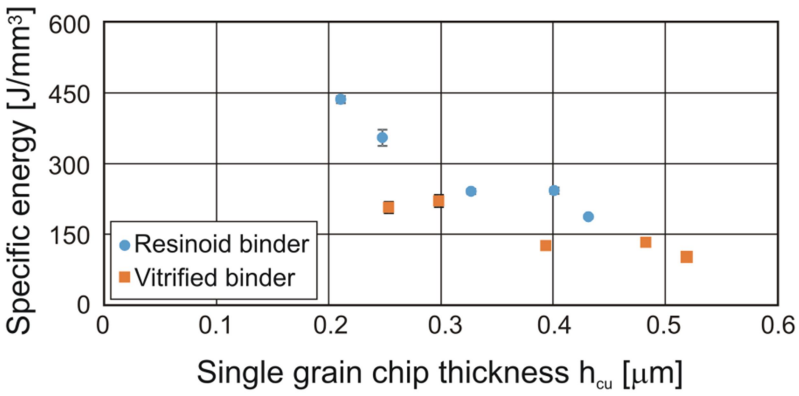

Fig. 8 Behavior of specific energy in relation to single grain chip thickness

Considering the behavior of the specific energy, it can be affirmed that higher chip thicknesses lead to the need of lower levels of energy consumption to remove a determined material volume. Thus, such parameter can be considered an indicator of grinding efficiency. However, higher values of chip thickness damage surface quality in the case of cemented tungsten carbide parts and, as a result, a balance between both effects should be met regarding a specific application.

5. Conclusion

This work investigated general aspects of plunge-face grinding WC-5%Co cutting inserts. From the obtained results, the following conclusions could be drawn:

-Through the measurement of the fraction of the abrasive surface which consists of peaks above the core material, it could be verified that the vitrified bonded wheel has 70% of the active edges of the resin bonded wheel.

-Such reduction of the number of active edges generates an increase in single grain chip thickness and contributes to an increase in surface roughness. Moreover, due to higher friction and temperature when in contact with cemented carbide, the vitrified bonded grinding wheel causes slightly higher values of surface and edge roughness in comparison to the resin bonded wheel.

-Surface roughness obtained after plunge-face grinding of cemented tungsten carbide is closer related to deeper valleys than higher peaks. In this regard, ploughing and smearing of the ground material do not play the most important role.

-Although lower values of specific energy are obtained, larger chip thicknesses lead to a brittle behavior of the material during its removal and damage surface quality. Otherwise, the influence of chip thickness on the edge roughness is not significant, because of an irregular removal of WC grains from the Co binder at this region, related to the low backing effect.

Acknowledgements

The authors would like to thank the Federal University of West Bahia (UFOB), the Brazilian Federal Agency for the Support and Evaluation of Graduate Education

(CAPES) and the Graduate Program in Materials Science and Engineering of the Federal University of São Carlos.

Funding: This work was supported by the São Paulo Research Foundation (FAPESP) (grant numbers 2015/15622-2, 2017/12309-7 and 2017/12304-5).

Conflict of Interest: The authors declare that they have no conflict of interest.

References

[1] Klocke F, König W (2005) Fertigungsverfahren – Schleifen, Honen, Läppen. 4th ed. Springer-Verlag, Berlin, Heidelberg (in German)

[2] Bifano TG, Dow TA, Scattergood RO (1991) Ductile-regime grinding: a new technology for machining brittle materials. J Eng Ind 133:184-189.

[3] Dai J, Su H, Yu T, Hu H, Zhou W, Ding W (2018) Experimental investigation on materials removal mechanism during grinding silicon carbide ceramics with single diamond grain. Prec Eng 51:271-279.

[4] Wu C, Li B, Liu Y, Liang SY (2017) Surface roughness modeling for grinding of silicon carbide ceramics considering co-existence of brittleness and ductility. Int J Mech Sci 133:167-177.

[5] Hegeman JBJW, De Hosson JThM, With G (2001) Grinding of WC-CO hardmetals. Wear 248:187-196.

[6] Ren YH, Zhang B, Zhou ZX (2009) Specific energy in grinding of tungsten carbides of various grain sizes. CIRP Ann Manuf Technol 58:299-302.

[7] Yang J, Roa JJ, Schwind M, Odén M, Johansson-Jõesaar MP, Esteve J, Llanes L (2016) Thermally induced surface integrity changes of ground WC-Co hardmetals. Proc CIRP 45:91-94.

[8] Yang J, Roa JJ, Schwind M, Odén M, Johansson-Jõesaar MP, Llanes L (2017) Grinding-induced metallurgical alterations in the binder phase of WC-Co cemented carbides. Mater Charact 134:302-310.

[9] Takeyama H, Iijima N, Uno K (1982) Surface integrity of cemented carbide tool and its brittle fracture. Ann CIRP 31:59-63.

[10] Yin L, Spowage AC, Ramesh K, Huang H, Pickering JP, Vancoille EYJ (2004) Influence of microstructure on ultraprecision grinding of cemented carbides. Int J Mach Tools Manuf 44:533-543.

[11] Klocke F, Wirtz C, Mueller S, Mattfeld P (2016) Analysis of the material behavior of cemented carbides (WC-Co) in grinding by single grain cutting tests. Proc CIRP 46:209-213.

[12] Badger J (2015) Grinding of sub-micron-grade carbide: contact and wear mechanisms, loading, conditioning, scrubbing and resin-bond degradation. CIRP Ann Manuf Technol 64:341-344.

[13] Zhan YJ, Xu XP (2012) An experimental investigation of temperatures and energy partition in grinding of cemented carbide with a brazed diamond wheel. Int J Adv Manuf Technol 61:117-125.

[14] Biermann D, Würz E (2009) A study of grinding silicon nitride and cemented carbide materials with diamond grinding wheels. Prod Eng Res Dev 3:411-416.

[15] Yin L, Pickering JP, Ramesh K, Huang H, Spowage AC, Vancoille EYJ (2005) Planar nanogrinding of a fine grained WC-Co composite for an optical surface finish. Int J Adv Manuf Technol 26:766-773.

[16] Abdullah A, Pak A, Farahi M, Barzegari M (2007) Profile wear of resin-bonded nickel-coated diamond wheel and roughness in creep-feed grinding of cemented tungsten carbide. J Mater Process Technol 183:165-168.

[17] Habrat WF (2016) Effect of bond type and process parameters on grinding force components in grinding of cemented carbide. Proc Eng 149:122-129.

[18] Friemuth T (1999) Schleifen hartstoffverstärkter keramischer Werkzeuge. Dr.-Ing. Dissertation, Universität Hannover. (in German)